

# Aeroelastic behavior of a slender body considering free fittings<sup>†</sup>

M. Ehramianpour<sup>1,\*</sup>, H. Haddadpour<sup>2</sup> and M. T. Ahmadian<sup>1</sup>

<sup>1</sup>*Faculty of Mechanical Engineering, Sharif University of Technology, Tehran, 11365-8639, Iran*

<sup>2</sup>*Faculty of Aerospace Engineering, Sharif University of Technology, Tehran, 11365-8639, Iran*

(Manuscript Received June 15, 2009; Revised January 11, 2010; Accepted May 21, 2010)

## Abstract

This paper presents dynamic and vibration analysis of a flight vehicle with consideration of the free fitting between its two sections. Using the Lagrangian approach, a general analytical model is developed for a non-spinning elastic vehicle in planar motion. The model contains rigid body motions and bending deformations of two sections of the flight vehicle and a nonlinear rotational spring that models the freeplay between the two sections. To express bending deformation, the mode summation method is applied. It is shown that freeplay in the joints significantly affects the trajectory of the flight vehicle. Numerical examples reveal the effect of a joint's nonlinearity on the trajectory and stability of the flight vehicle.

**Keywords:** Flight vehicle; Freeplay; Multi body; Nonlinear vibration

## 1. Introduction

Structural nonlinearities are subdivided into distributed nonlinearities and concentrated ones. Distributed nonlinearities are spread over the entire structure-like materials, but concentrated nonlinearities have a local effect in the control mechanism or the attachment of external stores. Most flight vehicles may have inherently concentrated structural nonlinearities such as freeplay, friction, hysteresis and preload in the hinged part of their control surfaces and sections. Among these nonlinearities, the freeplay usually results in the most critical flutter condition.

In this paper, a simulation of the response of a two-section flying flexible flight vehicle with initial conditions and external excitations is performed.

Linear flight mechanics of spinning projectiles was reformulated by Platus [1] in body-fixed coordinates for a general flight vehicle. Recently, with technological development of flight vehicles, effects of aeroelasticity have become a matter of possible concern for designers. Platus [2] developed a simple theory for elastically deforming flight vehicles. He assumed the elastic flight vehicle oscillates in the modal waveform of a nonspinning free-free beam whereas in uniform distribution of mass, the waveform is symmetric with equal deflections at each end. Bilimoria [3] established an integrated

approach for nonspinning elastic hypersonic flight vehicles. In order to predict the effect of flight vehicle flexibility on the control system, Newman [4] developed a two-dimensional aeroelastic model of flight vehicles. The effect of flexibility on the poles and zeros of a general flexible flight vehicle has been studied by Livneh and Schmidt [5]. Thrust effect in the boost phase of flight on the vibrational characteristics of flexible guided flight vehicles has also been studied by Pourakdoust and Assadian [6], numerically. Using the Lagrangian approach, Haddapour [7] studied the stability of a flight vehicle under the influence of a control loop on the aeroelastic system.

The effect of free fittings in a flight vehicle is not addressed well in the literature. This paper develops an analytical model for studying the aeroelasticity of a two-section flight vehicle with freeplay in rotation. For this purpose, component mode synthesis is used for elastic deflection, and slender body theorem is assumed for aerodynamic modeling. The solution of the equation of motion in time-domain is analyzed to study the effects of the free fittings under maximum altitude, range, and instability of the flight vehicle.

## 2. Formulation

### 2.1 Model definition

A two-section flexible flight vehicle with a torsional spring at joint, in a 2-D space is illustrated in Fig. 1. Each section of the flight vehicle has a body coordinate system originated at the joint and rotates with the appropriate section. The inertia frame is assumed to be at the flight starting point by which the

<sup>†</sup>This paper was recommended for publication in revised form by Associate Editor Eung-Soo Shin

\*Corresponding author. Tel.: +98 21 6616 4617, Fax.: +98 21 6602 2731  
E-mail address: m\_ehramian@yahoo.com

© KSME & Springer 2010

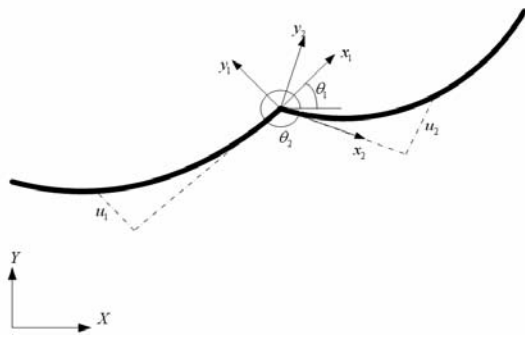


Fig. 1. The schematic view for flight vehicle.

relative displacement of the origin of the body coordinates is evaluated.

Elastic deflections of the flexible flight vehicle are treated as the motion of particles relative to the body-fixed axes of every section. Elastic deflections of every section  $u_i$  ( $i=1,2$ ) are assumed to be in the  $y$ -direction of the body-fixed coordinate for each section, and the length of the flight vehicle is assumed to be fixed for small bending deflections along the  $y$ -axes of each section. A torsional spring with coefficient  $K_\theta$  is used for modeling the joint between the two sections.

To derive the equations of motion, Lagrange's method is used. In general, Lagrange's equation is given by:

$$\frac{d}{dt} \left( \frac{\partial T}{\partial \dot{q}_i} \right) - \frac{\partial T}{\partial q_i} + \frac{\partial U}{\partial q_i} = Q_i \quad (1)$$

where  $q_i$ ,  $T$ ,  $U$ ,  $Q_i$  are generalized coordinates, kinetic energy, potential energy and generalized forces, respectively.

## 2.2 Structural model

For structural modeling, it is assumed that the elastic deformation of both sections of the flight vehicle is sufficiently small and can be represented in terms of normal modes of a cantilever beam. For a given mass element on the first section of the body, the elastic deformation may be expressed as

$$u_1(x, t) = \sum_{i=1}^n \phi_{1i}(x_1) \eta_{1i}(t) \quad (2)$$

and for the mass element on the second section of the body as

$$u_2(x, t) = \sum_{i=1}^n \phi_{2i}(x_2) \eta_{2i}(t) \quad (3)$$

where  $\phi_{1i}$  and  $\phi_{2i}$  are the bending normal modes of cantilevered beams of the first and second sections of the body, and  $\eta_{1i}$  and  $\eta_{2i}$  are the corresponding generalized coordinates, respectively. Using Euler beam theory,  $\phi_i$  must satisfy the following differential equation:

$$\frac{d^2}{dx^2} [E_j I_j \frac{d^2 \phi_{ji}(x_j)}{dx_j^2}] = -\Omega_{ji}^2 \phi_{ji}(x_j) \quad (4)$$

where  $E_j I_j(x_j)$  and  $m_j(x_j)$  are the beam flexural stiffness and mass distribution of the  $j^{\text{th}}$  section, respectively, and  $\Omega_{ji}$  is the  $i^{\text{th}}$  bending frequency of  $j^{\text{th}}$  section of the flight vehicle. Also the normal modes should also satisfy the orthogonality conditions which are:

$$\int_{L_j} \phi_{jk}(x_j) \phi_{jl}(x_j) m_j(x_j) dx_j = \begin{cases} 0, & k \neq l \\ M_k, & k = l \end{cases} \quad (5)$$

## 2.3 Kinetic energy

The body frames of the first and second section are fixed to the body of the flight vehicle in the joint point, and their  $x$  axes are tangent to the body in this point for every section. Let  $E_1$  and  $R_1$  be the position vectors of the mass element  $dm_1$  on the first section and joint point relative to the inertial axis, respectively. Vector  $r_1$  represents the position vector of the mass element  $dm_1$  relative to the body of the first frame. Thus, one can write the following relation for the mass element  $dm_1$  on the first section:

$$\vec{E}_1 = \vec{R}_1 + \vec{r}_1 = \vec{R}_1 + \vec{r}_{o1} + \vec{e}_1 \quad (6)$$

where  $e_1$  is the elastic deformation of the mass element and  $r_{o1}$  is the  $x$  distance of the mass element in body coordinate. The kinetic energy of the first part is given by:

$$T_1 = \frac{1}{2} \int \frac{dE_1}{dt} \cdot \frac{dE_1}{dt} dm_1. \quad (7)$$

Expanding Eq. 7 using Eq. 6 and defining  $\vec{V} = \frac{d\vec{R}}{dt}$  yields

$$T_1 = \frac{1}{2} m_1 V \cdot V + V \cdot \int \frac{dr_1}{dt} dm_1 + \frac{1}{2} \int \frac{dr_1}{dt} \cdot \frac{dr_1}{dt} dm_1 \quad (8)$$

Assuming constant mass and symmetry about the  $x$ -axis of the flight vehicle, after some manipulation, the final expression for the kinetic energy of the first section of the flight vehicle can be written as:

$$\begin{aligned} T = & \frac{1}{2} m_1 (\dot{X}^2 + \dot{Y}^2) - \dot{\theta}_1 (\dot{X} \cos(\theta_1) + \dot{Y} \sin(\theta_1)) (I_1 \dot{\eta}_1) + \\ & \frac{1}{2} \sum_{i=1}^n M_{1i} (\dot{\theta}_1^2 \eta_{1i}^2 + \dot{\eta}_{1i}^2) + (-\dot{X} \sin(\theta_1) + \dot{Y} \cos(\theta_1)) (I_1 \ddot{\eta}_1 - \dot{\theta}_1 G_1) \\ & + \frac{1}{2} I_{o1} \dot{\theta}_1^2 - \dot{\theta}_1 I_{1o} \ddot{\eta}_1 \end{aligned} \quad (9)$$

In Eq. 9,  $I_{o1}$ ,  $G_1$ ,  $I_{1i}$  and  $I_{1oi}$  are defined as follows:

$$I_{o1} = \int_{L_1} x_1^2 dm_1 \quad (10)$$

$$G_1 = \int_{L_1} x_1 dm_1 \quad (11)$$

$$I_{1i} = \int_L \phi_{1i}(x_1) dm_1 \quad (12)$$

$$I_{1\alpha i} = \int_L x_i \phi_{1i}(x_1) dm_1 \quad (13)$$

Using a similar manner for the second section, the overall kinetic energy of the system may be written as:

$$\begin{aligned} T = & \frac{1}{2}(m_1 + m_2)(\dot{X}^2 + \dot{Y}^2) \\ & - \dot{\theta}_1(\dot{X} \cos(\theta_1) + \dot{Y} \sin(\theta_1))(I_1 \dot{\eta}_1) \\ & - \dot{\theta}_2(\dot{X} \cos(\theta_2) + \dot{Y} \sin(\theta_2))(I_2 \dot{\eta}_2) \\ & + \frac{1}{2} \sum_{i=1}^n M_{1i} (\dot{\theta}_1^2 \eta_{1i}^2 + \dot{\eta}_{1i}^2) + \\ & \frac{1}{2} \sum_{i=1}^n M_{2i} (\dot{\theta}_2^2 \eta_{2i}^2 + \dot{\eta}_{2i}^2) + \\ & (-\dot{X} \sin(\theta_1) + \dot{Y} \cos(\theta_1))(I_1 \dot{\eta}_1 - \dot{\theta}_1 G_1) \\ & + (-\dot{X} \sin(\theta_2) + \dot{Y} \cos(\theta_2))(I_2 \dot{\eta}_2 + \dot{\theta}_2 G_2) \\ & + \frac{1}{2} I_{o1} \dot{\theta}_1^2 + \frac{1}{2} I_{o2} \dot{\theta}_2^2 - \dot{\theta}_1 I_{1\alpha} \dot{\eta}_1 + \dot{\theta}_2 I_{2\alpha} \dot{\eta}_2 \end{aligned} \quad (14)$$

## 2.4 Potential energy

Considering the effect of the gravity on the vehicle as an external force, the potential energy of the system may be written as:

$$\begin{aligned} U_e = & -\frac{1}{2} \int_{L_1} E_1 I_1 \left( \frac{\partial^2 u_1}{\partial x_1^2} \right) dx_1 \\ & -\frac{1}{2} \int_{L_2} E_2 I_2 \left( \frac{\partial^2 u_2}{\partial x_2^2} \right) dx_2 + \frac{1}{2} K_\theta (\theta_2 - \theta_1)^2 \end{aligned} \quad (15)$$

By combining Eqs. 4 and 15, the elastic potential energy may be written in terms of the generalized coordinates  $\eta_{1i}$ ,  $\eta_{2i}$  and modal natural frequencies  $\Omega_{1i}$ ,  $\Omega_{2i}$  as follows:

$$\begin{aligned} U_e = & \frac{1}{2} \sum_{i=1}^n M_{1i} \Omega_{1i}^2 \eta_{1i}^2 + \frac{1}{2} \sum_{i=1}^n M_{2i} \Omega_{2i}^2 \eta_{2i}^2 \\ & + \frac{1}{2} K_\theta (\theta_2 - \theta_1)^2 \end{aligned} \quad (16)$$

## 2.5 Equations of motion

Equations of motion may be derived using Lagrange's equation (Eq. 1). The equations of motion can be divided into force, moment and elastic deformation equations presented in Table 1.

Note that in these equations, the parameters  $\omega_1 = \dot{\theta}_1$ ,  $\omega_2 = \dot{\theta}_2$ ,  $\alpha_1 = \ddot{\theta}_1$  and  $\alpha_2 = \ddot{\theta}_2$  are used for simplicity.

## 2.6 Generalized forces

Generalized forces in Lagrange's equation can be represented using the principles of virtual work as follows:

Table 1. Equations of motions.

$(m_1 + m_2) \ddot{X} - (\alpha_1 \cos(\theta_1) - \omega_1^2 \sin(\theta_1))(I_1 \dot{\eta}_1)$
$- \omega_1 \cos(\theta_1)(I_1 \dot{\eta}_1) - (\alpha_2 \cos(\theta_2) - \omega_2^2 \sin(\theta_2))(I_2 \dot{\eta}_2)$
$- \omega_2 \cos(\theta_2)(I_2 \dot{\eta}_2) - \omega_1 \cos(\theta_1)(I_1 \dot{\eta}_1 - \omega_1 G_1)$
$- \sin(\theta_1)(I_1 \dot{\eta}_1 - \alpha_1 G_1) - \omega_2 \cos(\theta_2)(I_2 \dot{\eta}_2 + \omega_2 G_2)$
$- \sin(\theta_2)(I_2 \dot{\eta}_2 + \alpha_2 G_2) = Q_x$
$(m_1 + m_2) \ddot{Y} - (\alpha_1 \sin(\theta_1) + \omega_1^2 \cos(\theta_1))(I_1 \dot{\eta}_1)$
$- \omega_1 \sin(\theta_1)(I_1 \dot{\eta}_1) - (\alpha_2 \sin(\theta_2) + \omega_2^2 \cos(\theta_2))(I_2 \dot{\eta}_2)$
$- \omega_2 \sin(\theta_2)(I_2 \dot{\eta}_2) - \omega_1 \sin(\theta_1)(I_1 \dot{\eta}_1 - \omega_1 G_1) +$
$\cos(\theta_1)(I_1 \dot{\eta}_1 - \alpha_1 G_1) - \omega_2 \sin(\theta_2)(I_2 \dot{\eta}_2 + \omega_2 G_2)$
$+ \cos(\theta_2)(I_2 \dot{\eta}_2 + \alpha_2 G_2) = Q_y$
$- (\ddot{X} \cos(\theta_1) + \ddot{Y} \sin(\theta_1))(I_1 \dot{\eta}_1) + \sum_{i=1}^n M_{1i} (\alpha_1 \eta_{1i}^2 + 2\omega_1 \eta_{1i} \dot{\eta}_{1i})$
$- G_1 (-\ddot{X} \sin(\theta_1) + \ddot{Y} \cos(\theta_1)) + I_{o1} \alpha_1 - I_{1\alpha} \ddot{\eta}_1 +$
$K_\theta (\theta_2 - \theta_1) = Q_{\theta_1}$
$- (\ddot{X} \cos(\theta_2) + \ddot{Y} \sin(\theta_2))(I_2 \dot{\eta}_2) + \alpha_2 \sum_{i=1}^n M_{2i} \eta_{2i}^2 +$
$\omega_2 \sum_{i=1}^n M_{2i} (2\eta_{2i} \dot{\eta}_{2i}) + G_2 (-\ddot{X} \sin(\theta_2) + \ddot{Y} \cos(\theta_2))$
$+ I_{o2} \alpha_2 + I_{2\alpha} \ddot{\eta}_2 + K_\theta (\theta_2 - \theta_1) = Q_{\theta_2}$
$M_{1i} \ddot{\eta}_{1i} + (-\ddot{X} \sin(\theta_1) + \ddot{Y} \cos(\theta_1)) I_{1i} - \alpha_1 I_{1\alpha i}$
$- \omega_1^2 M_{1i} \eta_{1i} + E_1 I_1 \int_0^{l_1} \phi''_{1i}(x_1) \sum_{j=1}^n \phi''_{1j}(x_1) \eta_{1j} dx_1 = Q_{\eta_{1i}}$
$M_{2i} \ddot{\eta}_{2i} + (-\ddot{X} \sin(\theta_2) + \ddot{Y} \cos(\theta_2)) I_{2i} + \alpha_2 I_{2\alpha i}$
$- \omega_2^2 M_{2i} \eta_{2i} + E_2 I_2 \int_0^{l_2} \phi''_{2i}(x_2) \sum_{j=1}^n \phi''_{2j}(x_2) \eta_{2j} dx_2 = Q_{\eta_{2i}}$

$$Q_i = \frac{\partial (\delta W)}{\partial (\delta q_i)} \quad (17)$$

Here  $\delta W$  is the virtual work done during a virtual displacement along the generalized coordinates,  $\delta q_i$ . The virtual work is the summation of the work done by the pressure distribution during the rigid body translation and rotation, the elastic deformation of the vehicle,  $\delta W_1$ , and the work done by the thrust,  $\delta W_2$ . Hence using the notations of Ref. [6], the first part of the virtual work can be written as:

$$\begin{aligned} \delta W_1 = & \int_{S1} [(P - P_\infty) n' dA] \cdot [\delta \vec{R}'_1 + \delta \vec{U}'_1] \\ & + \int_{S1} [\vec{r}_o \times (P - P_\infty) n' dA] \cdot [\delta \vec{F}'_1] \\ & \int_{S2} [(P - P_\infty) n' dA] \cdot [\delta \vec{R}'_2 + \delta \vec{U}'_2] \\ & + \int_{S2} [\vec{r}_o \times (P - P_\infty) n' dA] \cdot [\delta \vec{F}'_2] \end{aligned} \quad (18)$$

where A is the body surface area of the flight vehicle,  $n'$  is the inward-pointing unit vector normal to the surface at every

point and  $s_1, s_2$  are the deformed lengths of the first and second sections of the flight vehicle. The linearized pressure distribution on the body leads to:

$$\text{for } s_1 \rightarrow (P - P_{\infty})n'dA = L_{\alpha 1}(x_1)\alpha_1(x_1, t)[-\sin(\theta_1)\vec{i} + \cos(\theta_1)\vec{j}]dx_1 \quad (19)$$

$$\text{for } s_2 \rightarrow (P - P_{\infty})n'dA = L_{\alpha 2}(x_2)\alpha_2(x_2, t)[-\sin(\theta_2)\vec{i} + \cos(\theta_2)\vec{j}]dx_2 \quad (20)$$

where  $L_{\alpha 1}$  and  $L_{\alpha 2}$  are the lift curve derivatives,  $\alpha_1(x_1, t)$  and  $\alpha_2(x_2, t)$  are the local angles of attack, and  $\delta R_1$  and  $\delta R_2$  are the virtual displacement vectors of every mass element of the first and second sections, respectively. To write the second part of the virtual work, the expression for the thrust force vector must be written as:

$$\vec{F}_{Th} = F_{Th}(\cos(\theta_3)i + \sin(\theta_3)j) \quad (21)$$

where  $\theta_3$  is the tangential angle of the vehicle thrust, as shown below:

$$\theta_3 = \theta_i + \frac{\partial u_i(x_i)}{\partial x_i} \Big|_{l_i} + \theta_0 \sin(\omega t) \quad (22)$$

The displacement vector may be written as:

$$\delta r_{F_{Th}} = \delta(Xi + Yj + l_1(-\cos(\theta_1)i - \sin(\theta_1)j) + u_1(l_1)(-\sin(\theta_1)i + \cos(\theta_1)j)) \quad (23)$$

By substituting Eq. 23 into Eq. 22, the virtual work done by the thrust force can be obtained as follows:

$$\begin{aligned} \delta W_2 &= F_{Th} \cdot \delta r_F = F_{Th} \cos(\theta_3) \delta X + F_{Th} \sin(\theta_3) \delta Y \\ &\quad + F_{Th} \delta u_1(l_1) \sin(\theta_3 - \theta_1) + \\ &\quad \delta \theta_1 (-F_{Th} u_1(l_1) \cos(\theta_1 - \theta_3) - F_{Th} \sin(\theta_3 - \theta_1)) \end{aligned} \quad (24)$$

## 2.7 Angles of attack

The angle of attack at any point on every section is the summation of its rigid body values  $\alpha_1$  and  $\alpha_2$ , the local bending slopes  $u'_1$  and  $u'_2$ , the damping terms arising from the deflection rates  $u_1$  and  $u_2$ , and the body angular rates  $\omega_1$  and  $\omega_2$  may be written as [2]

$$\alpha_1(x_1, t) = \alpha_1 - \frac{dU_1(x_1)}{dx_1} + \frac{-\dot{U}_1(x_1) + \omega_1 x_1}{V_t} \quad (25)$$

$$\alpha_2(x_2, t) = \alpha_2 + \frac{dU_2(x_2)}{dx_2} + \frac{-\dot{U}_2(x_2) - \omega_2 x_2}{V_{t_2}} \quad (26)$$

Inserting Eqs. 2 and 3 into Eqs. 25 and 26 one gets

Table 2. Generalized forces.

$Q_x = \frac{1}{2} \rho_{\infty} S$	$\left\{ \begin{array}{l} U_1^2 \sin(\theta_1) \left\{ \begin{array}{l} -\left( -\frac{V_1}{U_1} + \theta_1 \right) L_{\alpha 1} + \sum_{i=1}^n R_i^1 \eta_{1i} \\ + \frac{\sum_{i=1}^n P_i^1 \dot{\eta}_{1i} - \omega_1 M_{\alpha 1}}{U_1} \end{array} \right\} + \\ U_1^2 \sin(\theta_2) \left\{ \begin{array}{l} -\left( -\frac{V_2}{U_2} + \theta_2 \right) L_{\alpha 2} - \sum_{i=1}^n R_i^2 \eta_{2i} \\ + \frac{\sum_{i=1}^n P_i^2 \dot{\eta}_{2i} + \omega_2 M_{\alpha 2}}{U_2} \end{array} \right\} \\ + F_{Th} \cos(\theta_3) \end{array} \right\}$
$Q_y = \frac{1}{2} \rho_{\infty} S$	$\left\{ \begin{array}{l} U_1^2 \cos(\theta_1) \left\{ \begin{array}{l} \left( -\frac{V_1}{U_1} + \theta_1 \right) L_{\alpha 1} - \sum_{i=1}^n R_i^1 \eta_{1i} \\ + \frac{-\sum_{i=1}^n P_i^1 \dot{\eta}_{1i} + \omega_1 M_{\alpha 1}}{U_1} \end{array} \right\} + \\ U_2^2 \cos(\theta_2) \left\{ \begin{array}{l} \left( -\frac{V_2}{U_2} + \theta_2 \right) L_{\alpha 2} + \sum_{i=1}^n R_i^2 \eta_{2i} \\ - \frac{\sum_{i=1}^n P_i^2 \dot{\eta}_{2i} + \omega_2 M_{\alpha 2}}{U_2} \end{array} \right\} \\ + F_{Th} \sin(\theta_3) \end{array} \right\}$
$Q_{\theta_1} = \frac{1}{2} \rho_{\infty} U_1^2 S$	$\left\{ \begin{array}{l} \left( -\frac{V_1}{U_1} + \theta_1 \right) M_{\alpha 1} + \sum_{i=1}^n S_i^1 \eta_{1i} \\ + \frac{\sum_{i=1}^n Q_i^1 \dot{\eta}_{1i} - \omega_1 J_{\alpha 1}}{U_1} \\ + F_{Th} l_1 \sin(\theta_1 - \theta_3) - F_{Th} u_1(l_1) \cos(\theta_1 - \theta_3) \end{array} \right\}$
$Q_{\theta_2} = \frac{1}{2} \rho_{\infty} U_2^2 S$	$\left\{ \begin{array}{l} \left( -\frac{V_2}{U_2} + \theta_2 \right) M_{\alpha 2} + \sum_{i=1}^n S_i^2 \eta_{2i} \\ - \frac{\sum_{i=1}^n Q_i^2 \dot{\eta}_{2i} + \omega_2 J_{\alpha 2}}{U_2} \end{array} \right\}$
$Q_{\eta_{1i}} = \frac{1}{2} \rho_{\infty} U_1^2 S$	$\left\{ \begin{array}{l} \left( -\frac{V_1}{U_1} + \theta_1 \right) P_i^1 - \sum_{j=1}^n u_j^1 \eta_{1j} + \\ - \frac{\sum_{j=1}^n t_{ij}^1 \dot{\eta}_{1j} + \omega_1 Q_i^1}{U_1} \\ + F_{Th} \phi_{l_1}(l_1) \sin(\theta_3 - \theta_1) \end{array} \right\}$
$Q_{\eta_{2i}} = \frac{1}{2} \rho_{\infty} U_2^2 S$	$\left\{ \begin{array}{l} \left( -\frac{V_2}{U_2} + \theta_2 \right) P_i^2 + \sum_{j=1}^n u_j^2 \eta_{2j} \\ - \frac{\sum_{j=1}^n t_{ij}^2 \dot{\eta}_{2j} + \omega_2 Q_i^2}{U_2} \end{array} \right\}$

Table 1. Required Equations and Integrals in Table 2.

$U_1 = \dot{X} \cos(\theta_1) + \dot{Y} \sin(\theta_1)$
$U_2 = \dot{X} \cos(\theta_2) + \dot{Y} \sin(\theta_2)$
$V_1 = -\dot{X} \sin(\theta_1) + \dot{Y} \cos(\theta_1)$
$V_2 = -\dot{X} \sin(\theta_2) + \dot{Y} \cos(\theta_2)$
$L_{\alpha 1} = \int_{s_1} L_{\alpha 1}(x_1) dx_1$
$L_{\alpha 2} = \int_{s_2} L_{\alpha 2}(x_2) dx_2$
$M_{\alpha 1} = \int_{s_1} x_1 L_{\alpha 1}(x_1) dx_1$
$M_{\alpha 2} = \int_{s_2} x_2 L_{\alpha 2}(x_2) dx_2$
$J_{\alpha 1} = \int_{s_1} x_1^2 L_{\alpha 1}(x_1) dx_1$
$J_{\alpha 2} = \int_{s_2} x_2^2 L_{\alpha 2}(x_2) dx_2$
$P_i^1 = \int_{s_1} L_{\alpha 1}(x_1) \phi_{1i}(x_1) dx_1$
$P_i^2 = \int_{s_2} L_{\alpha 2}(x_2) \phi_{2i}(x_2) dx_2$
$Q_i^1 = \int_{s_1} x_1 L_{\alpha 1}(x_1) \phi_{1i}(x_1) dx_1$
$Q_i^2 = \int_{s_2} x_2 L_{\alpha 2}(x_2) \phi_{2i}(x_2) dx_2$
$R_i^1 = \int_{s_1} L_{\alpha 1}(x_1) \phi'_{1i}(x_1) dx_1$
$R_i^2 = \int_{s_2} L_{\alpha 2}(x_2) \phi'_{2i}(x_2) dx_2$
$S_i^1 = \int_{s_1} x_1 L_{\alpha 1}(x_1) \phi'_{1i}(x_1) dx_1$
$S_i^2 = \int_{s_2} x_2 L_{\alpha 2}(x_2) \phi'_{2i}(x_2) dx_2$
$t_{ij}^1 = \int_{s_1} L_{\alpha 1}(x_1) \phi_{1i}(x_1) \phi_{1j}(x_1) dx_1$
$t_{ij}^2 = \int_{s_2} L_{\alpha 2}(x_2) \phi_{2i}(x_2) \phi_{2j}(x_2) dx_2$
$u_{ij}^1 = \int_{s_1} L_{\alpha 1}(x_1) \phi_{1i}(x_1) \phi'_{1j}(x_1) dx_1$

$$\alpha_1(x_1, t) = \alpha_1 - \sum_{i=1}^n \phi'_{1i}(x_1) \eta_{1i} - \sum_{i=1}^n \phi_{1i}(x_1) \dot{\eta}_{1i} + \omega_1 x_1 + \frac{-\sum_{i=1}^n \phi_{1i}(x_1) \dot{\eta}_{1i} + \omega_1 x_1}{V_t} \quad (27)$$

$$\alpha_2(x_2, t) = \alpha_2 + \sum_{i=1}^n \phi'_{2i}(x_2) \eta_{2i} - \sum_{i=1}^n \phi_{2i}(x_2) \dot{\eta}_{2i} - \omega_2 x_2 + \frac{-\sum_{i=1}^n \phi_{2i}(x_2) \dot{\eta}_{2i} - \omega_2 x_2}{V_t} \quad (28)$$

Table 2. Required data for test case.

Parameter	Value	Unit
$m_1$	25	Kg
$m_2$	75	Kg
$l_1$	2.5	M
$l_2$	2.5	M
$E_1 I_1$	$3.33 \times 10^5$	N.m <sup>2</sup>
$E_2 I_2$	$3.33 \times 10^5$	N.m <sup>2</sup>
$G_1$	31.25	kg.m
$G_2$	93.75	kg.m
$I_{01}$	52	Kg.m <sup>2</sup>
$I_{02}$	156	Kg.m <sup>2</sup>

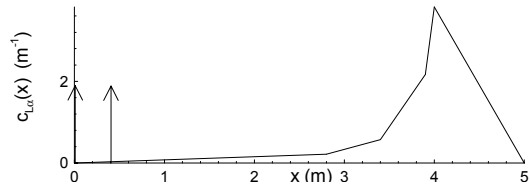


Fig. 2. Lift coefficient distribution along length [7].

where  $\alpha_1$  and  $\alpha_2$  are:

$$\alpha_1 = -\frac{-\dot{X} \sin(\theta_1) + \dot{Y} \cos(\theta_1)}{\dot{X} \cos(\theta_1) + \dot{Y} \sin(\theta_1)} + \theta_1 \quad (29)$$

$$\alpha_2 = -\frac{-\dot{X} \sin(\theta_2) + \dot{Y} \cos(\theta_2)}{\dot{X} \cos(\theta_2) + \dot{Y} \sin(\theta_2)} + \theta_2 \quad (30)$$

Using Eqs. 29 and 30 along with Eqs. 19 and 20, we obtain the generalized forces as shown in Table 2.

In these equations,  $\rho_\infty$  and  $S$  are air density and reference area, respectively. The symbols used in Table 2 are defined in Table 3. With the generalized forces, the governing equations of motion are completed and can be solved to determine stability and aeroelastic response.

### 3. Numerical results

In order to demonstrate the validity of the model, the aeroelastic stability is examined using a test case. Let the test case parameters be as shown in Fig. 2 and given in Table 4.

Results of the Eigenvalues of the linearized system versus air velocity using two modes of bending, and the results given by Haddapour [7] are presented in Figs. 3(a) and 3(b). In this problem, the coefficient of the spring is considered to be constant with the value of  $6 \times 105$  N.m/Rad. Numerical values of divergence velocity are also presented in Table 5. A 1.4% difference between the numerical values of velocity divergence clearly indicates the accuracy of the method.

Table 3. Specific values for the test case.

Method	Divergence Velocity (m/s)
Method of Ref [7]	2511
Present Work	2475

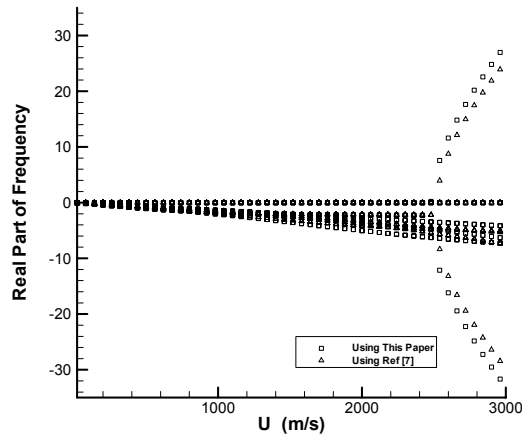


Fig. 3. (a) Frequency of the flight vehicle as a function of the flight vehicle Velocity U.

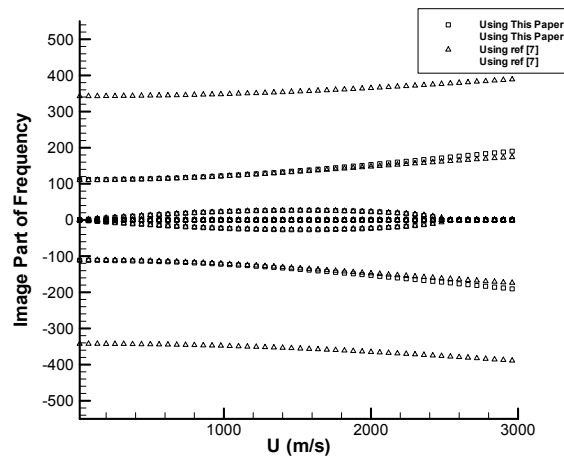


Fig. 3. (b) Frequency of the flight vehicle as a function of the flight vehicle Velocity U.

### 3.1 Results with freeplay

In the next step, the spring is modeled to have a freeplay angle as shown in Fig. 4. As indicated in this figure for modeling the freeplay of the joint, the coefficient of the spring,  $K_\theta$ , for an interval of angle,  $\delta$ , between two sections is assumed to be zero, and for larger angles,  $K_\theta$  has a value equal to  $6 \times 10^5$  N.m/Rad while the freeplay angle should be 0.2.

The trajectory of the flight vehicle using different numbers of modes for modeling the elasticity of the vehicle is presented in Fig. 5. The values of the initial velocity is assumed to be 400 m/s, the initial horizontal angle of the flight vehicle, 45°, and the thrust force of 30000 N exerted at the end of the first sec-

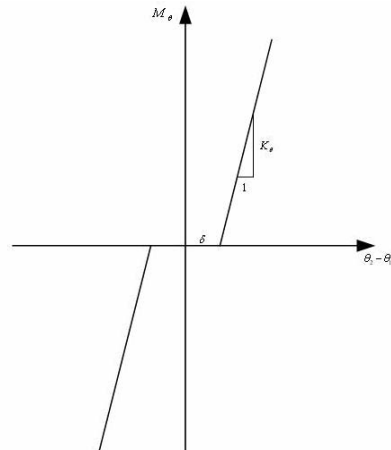


Fig. 4. Nonlinear spring force as a function of the angle between two sections.

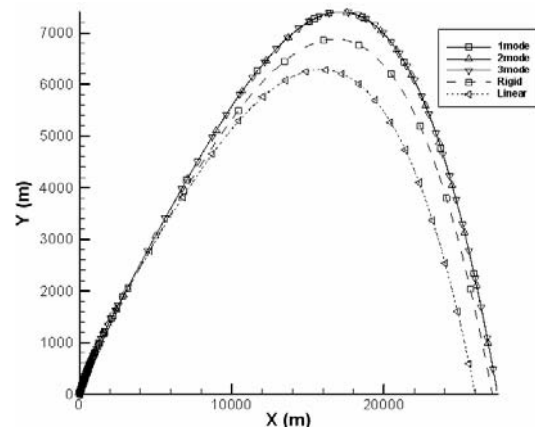


Fig. 5. Freepay effect on the trajectory of the elastic projectile using different mode.

tion during the first five-second interval of the flight. In this figure, the trajectory of the vehicle with two rigid sections and a nonlinear spring along with two elastic sections with a linear spring is also presented.

As shown in this figure, the trajectory after applying one, two and three modes for elastic deflection are very close to one another. Comparing the results of the rigid model with a nonlinear spring and the elastic model with a nonlinear spring shows an approximate difference in the trajectory ~2% in the range--while comparing the elastic model with linear and nonlinear springs results in a 5.5% difference in range. Results also show that the effect of the number of modes applied to the system is negligible on the range and trajectory. On this basis, only two elastic modes are applied to the system.

Freepay and initial conditions play important roles in the dynamics of the flight vehicle. Table 6 shows the results for the different simulations of flight with and without freepay. In these simulations, the initial velocity of the flight vehicle is assumed to be 400 m/s and the initial angle between two sec-

Table 6. Flight characteristics with different initial angles.

$\Theta_0$	With Nonlinear Spring ( $\delta=2^\circ$ )			With Linear Spring ( $\delta=0^\circ$ )		
	Range (m)	Max Height (m)	Time (s)	Range (m)	Max Height (m)	Time (s)
10.0	15277.9	567.7	25.7	11572.9	376.3	18.1
20.0	22172.7	2079.8	45.5	19102.5	1544.3	36.1
30.0	25602.1	4048.9	61.4	23292.2	3237.6	51.8
40.0	27198.7	6278.7	75.1	25472.1	5231.6	65.6
50.0	27511.9	8561.4	86.7	26251.1	7344.9	77.5
60.0	26943.8	10722.2	96.3	25047.3	11223.4	95.5

Table 7. Flight characteristics for different angles between two sections.

	X <sub>end</sub> (m)	Y <sub>max</sub> (m)	t <sub>end</sub> (s)	$\Theta_{\text{end}}$ (deg)
$\delta\theta_0 = -1.0$	17608	3023	37	-22
$\delta\theta_0 = -0.8$	17612	3022	37	-22
$\delta\theta_0 = -0.6$	17771	3089	38	-22
$\delta\theta_0 = -0.4$	17712	3062	37	-22
$\delta\theta_0 = -0.2$	31054	15193	127	-32
$\delta\theta_0 = 0.0$	31013	15460	128	-32
$\delta\theta_0 = 0.2$	31044	15343	127	-32
$\delta\theta_0 = 0.4$	31040	15516	128	-32
$\delta\theta_0 = 0.6$	31066	15518	128	-32
$\delta\theta_0 = 0.8$	31076	15476	128	-32
$\delta\theta_0 = 1.0$	31018	15546	128	-32

tions is zero.

As indicated in Table 5, the time and the range of the flight depend very much on the freeplay angle.

To evaluate the effect of the initial angle between two sections, the following initial conditions are employed and the results are presented in Table 7. The thrust force, initial velocity of the flight vehicle, and the initial angle of the flight vehicle with the horizontal line are the same as those in the previous example and  $\delta$  is equal to 1 degree. Note that the angle of the freeplay is assumed to be large enough to differentiate the effect of this angle on the dynamics of the flight.

The time and range of the flight with freeplay depends completely on the final angle between two sections at upper or lower limit.

For the initial angle between two sections of  $-0.8^\circ$ , the phase space related to the angle between two sections is plotted in Fig. 6.

As shown in this figure, the state of the system depending on the initial conditions switches between two regions of negative or positive limit. Removing the thrust force and

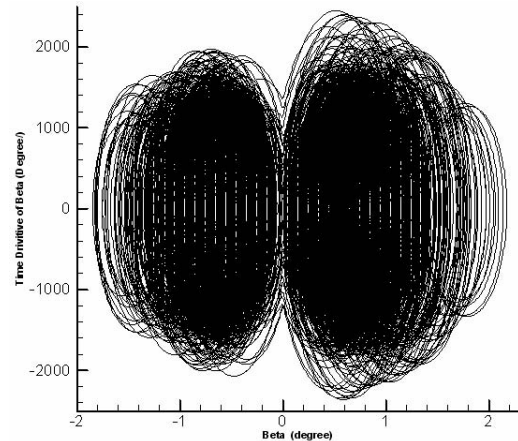


Fig. 6. Phase space for the angle between two sections.

dampening the initial conditions causes the state to remain in close contact with the related region. By continuing simulation, the state of the system would circulate about one of the two points and the energy of the system would gradually dampen.

#### 4. Conclusion

Equations of motion for flight of a two-section flight vehicle with freeplay are developed using slender body aerodynamic theory and component mode synthesis for bending deformation. It is shown that freeplay between two sections strongly affects the flight of the vehicle. The duration, range and maximum height of the flight vehicle depend on the initial conditions of the flight. Changing one of the initial conditions changes the characteristics of the flight due to the nonlinear nature of the freeplay. During the flight, the angle between two sections of the flight vehicle switches between the two limits of the fitting and eventually remains closer to one of them. Finally, it has been observed that the dynamics of the flight depend on the number of the assumed modes due to the nonlinear nature of the applied equations and approximations implemented in the problem.

#### References

- [1] D. H. Platus, Ballistic Re-Entry Vehicle Dynamics, *Journal of Guidance and Control*, 5 (1) (1982) 4-16.
- [2] D. H. Platus, Aeroelastic Stability of Slender, Spinning Missiles, *Journal of Guidance, Control, and Dynamics*, 15 (1) (1992) 144-151.
- [3] K. D. Bilimoria and D. K. Schmidt, Integrated development of the equation of motion for elastic hypersonic elastic vehicles, *J. Guidance, Control and Dynamics*, 18 (1) (1995).
- [4] B. Newman and D. K. Schmidt, Numerical and Literal Aeroelastic-Vehicle-Model Reduction for Feedback control Synthesis, *Journal of Guidance, Control, and Dynamics*, 14 (5) (1991) 943-953.

- [5] R. Livneh and D. K. Schmidt, Unified literal approximations for longitudinal dynamics of flexible vehicles, *Journal of Guidance, Control, and Dynamics*, 18 (5) (1995) 1074-1083.
- [6] S. H. Pourtakdoust and N. Assadian, Aeroelastic analysis of guided hypersonic launch vehicles, *J. Sound and Vibration*, 272 1-2.
- [7] H. Haddadpour, Aerostervoelastic stability of supersonic slender body flight vehicles, *J. Guidance, Control, Dynamics*, 29 (6) (2006) 1423-1427.



**Mostafa Ehramianpour** received a B.Sc. degree in mechanical engineering from the Amirkabir University of Tehran, Iran in 2005. He also graduated from the M.Sc. degree program for mechanical engineering in the applied design course from the Sharif University of Technology. His research focuses on the control Theorem, Flight Dynamics and Multibody Vibration.